Journal of Neuroscience Methods 132 (2004) 199–208

JOURNAL OF NEUROSCIENCE METHODS

www.elsevier.com/locate/jneumeth

PET Measurement of rCBF in the presence of a neurochemical tracer

Alexander K. Converse [a,*], Todd E. Barnhart [b], Kevin A. Dabbs [b], Onofre T. DeJesus [b], Julie A. Larson [c], Robert J. Nickles [b], Mary L. Schneider [d], Andrew D. Roberts [b,e]

[a] *Keck Laboratory for Functional Brain Imaging, University of Wisconsin, T-121 Waisman Center, 1500 N. Highland Avenue, Madison, WI 53705, USA*
[b] *Department of Medical Physics, University of Wisconsin, Madison, WI, USA*
[c] *Harlow Center for Biological Psychology, University of Wisconsin, Madison, WI, USA*
[d] *Department of Kinesiology, University of Wisconsin, Madison, WI, USA*
[e] *Department of Psychiatry, University of Wisconsin, Madison, WI, USA*

Received 14 April 2003; received in revised form 21 July 2003; accepted 12 September 2003

Abstract

Functional neurochemical imaging can indicate neurotransmitter release by detecting changes in receptor occupancy. A dual tracer positron emission tomography (PET) technique is presented here to extend such studies by simultaneously measuring changes in regional cerebral blood flow (rCBF). This would permit correlations of task or drug induced changes in rCBF and neurochemical function. In this proposed method, the rapidly varying signal from a blood flow tracer is distinguished from the slowly changing signal due to a long-lived neurochemical tracer. As a proof of principle, baseline studies were carried out in rhesus monkeys. Two monkeys were anesthetized with isoflurane, and [^{18}F]fallypride ($t_{1/2}$ = 110 min), a dopamine D2 receptor antagonist, was injected. Starting 99–137 min after injection, PET images were acquired every 10 s while the blood flow tracer [^{17}F]fluoromethane ($t_{1/2}$ = 65 s) was administered by inhalation in a repeating pattern of 45 s on/45 s off. The observed time–activity curves for 2 ml brain regions were fit with a three compartment lung–body–brain model of fluoromethane kinetics with whole brain perfusion fixed. Comparing consecutive 6 min scans, reproducibility of relative rCBF and striatal [^{18}F]fallypride concentration were 9 and 8%, respectively.

Keywords: Dopamine release; Neuromodulation; [^{11}C]raclopride

1. Introduction

Functional imaging of neurochemistry serves as a valuable tool in understanding the roles of specific neurotransmitters. Positron emission tomography (PET) and single photon emission computed tomography (SPECT) have been used to map brain circuitry that relies on a given neurotransmitter and to evaluate drugs that target a particular neurotransmission system. Radioactive tracers have been used to image different aspects of neurotransmission, including neurotransmitter production and receptor occupancy, and changes in synaptic neurotransmitter levels can be inferred from measured differences in binding of radiolabeled neuroreceptor ligands (Laruelle, 2000). Using [^{11}C]raclopride in humans, PET studies have examined striatal dopamine release in response to pharmacological challenges, tasks, and placebo (de la Fuente-Fernández et al., 2001; Koepp et al., 1998; Volkow et al., 1994). A PET study using sequential scans with [^{15}O]water and 6-[^{18}F]DOPA correlated prefrontal cortex blood flow and striatal dopamine synthesis in humans performing a task (Meyer-Lindenberg et al., 2002). Because of within-subject variation between scans, e.g. due to habituation, it would be valuable to image neurochemical function and blood flow alteration simultaneously. For example, it would be illuminating to image the nigrostriatal dopamine circuit by observing correlations between striatal dopamine release and blood flow alterations in midbrain and motor cortex during a motor task. Similarly, the mesolimbic dopamine circuit could be imaged during an attention task.

A number of techniques might permit such simultaneous measurements of rCBF and a neurochemical tracer. Transport from plasma to tissue of a long-lived neurochemical tracer with high permeability is itself blood flow dependent, so analysis of a single tracer scan with a compartmental

* Corresponding author. Tel.: +1-608-265-6604.
E-mail address: akconverse@wisc.edu (A.K. Converse).

0165-0270/$ – see front matter © 2003 Elsevier B.V. All rights reserved.
doi:10.1016/j.jneumeth.2003.09.006

model provides a measure of rCBF (Logan et al., 1994). SPECT has been used to distinguish a blood flow tracer and a neurochemical tracer based on the energies of their emitted photons (El Fakhri et al., 2001). PET detectors have been successfully operated within the bore of a magnetic resonance imaging (MRI) scanner, which might permit simultaneous observation of a PET neurochemical tracer and blood flow dependent MRI parameters (Slates et al., 1999).

Here we propose a PET method to image neurochemical function simultaneously with regional blood flow dynamics, in which a short lived blood flow tracer is delivered in the presence of a long-lived neurochemical tracer. The rapidly varying temporal pattern in the blood flow tracer signal can then be distinguished from the signal due to the neurochemical tracer, which changes over a longer time scale. Simultaneous dual tracer PET studies of equilibrated tracers, which rely on the difference in radioactive half lives, have been performed in phantoms (Huang et al., 1982) and proposed for humans (Kearfott, 1990). Separation of signals from long-lived tracers based on physiological kinetics has been achieved by staggered injections of pairs of ^{11}C labeled tracers (Koeppe et al., 2001), but repeated measures of blood flow over the course of a neurochemical scan require the use of a short lived tracer. An attempt has been made to simultaneously image [^{15}O]water during a [^{11}C]neuroreceptor ligand study in humans (unpublished data) (Koeppe, 2003).

The measurement reported here is intended as a proof of principle. In this study, we do not search for changes in neurochemistry or rCBF, rather we assess the reproducibility of baseline measurements.

2. Methods

2.1. Radioactive tracers

[^{18}F]fallypride ($t_{1/2}$ = 110 min) was prepared using the method of Mukherjee et al. (1997). Fallypride is a high affinity dopamine D2 receptor antagonist, which has been shown to be insensitive to small fluctuations in dopamine levels, making it a stable neurochemical tracer for this baseline study (Mukherjee et al., 1997). To measure blood flow, the inert freely diffusible tracer [^{17}F]fluoromethane (CH_3F, $t_{1/2}$ = 64.5 s) was produced with an in-line gas phase method (Dabbs et al., 2001).

2.2. Subjects

Three healthy juvenile rhesus monkeys were studied (*Macaca mulatta*, 2 F/1 M, 4.8–6.4 kg). Fifty to sixty-five minutes prior to radiotracer delivery, the monkeys were anesthetized with ketamine (15 mg/kg i.m.) for intubation and transport. Upon arrival at the PET scanner, they were placed on 1.25% isoflurane in oxygen. For radiotracer injection, a catheter was inserted into the saphenous vein and a central line was run to the vena cava. The monkeys' heart rate, SpO_2, respiratory rate, and temperature were monitored during scanning. These studies were conducted with the approval of the University of Wisconsin, Madison Animal Care and Use Committee.

2.3. Scans

PET scans were performed with an ECAT 933/04 tomograph (CTI, Knoxville, TN). The scanner has a 52 mm axial field of view with 7.4 mm axial image plane separation. The reconstructed image resolution is 5.4 mm FWHM transaxial and 6.4 mm FWHM axial (Sunderland and Nickles, 1988). Anesthetized monkeys were positioned on their left side, and their heads were secured to the bed with tape to prevent motion. Seven axial slices were acquired covering the range 33 mm superior to 19 mm inferior to the orbital–metal plane.

Prior to administration of tracers, a 5 min transmission scan was performed. For two subjects (monkeys 2 and 3), [^{18}F]fallypride was then injected (189 and 78 MBq). A 90 min scan (5 frames × 2 min + 8 frames × 10 min) was begun at injection. Following the scan with [^{18}F]fallypride alone dual tracer scans were acquired, during which [^{17}F]fluoromethane was administered by inhalation (17 MBq/s in 2 ml/s neon) in a repeating pattern of 45 s on/45 s off ("modulated delivery"). During the on phase, [^{17}F]fluoromethane was added to the breathing tube approximately 10 cm from the mouth. During the off phase, [^{17}F]fluoromethane was vented. Data with both tracers present were acquired in two 12 min scans (72 frames × 10 s), which were begun 99–137 min after injection of [^{18}F]fallypride. Dual tracer scans were preceded by ca. 3 min of continuous [^{17}F]fluoromethane delivery, and scans started with the onset of modulated delivery. The [^{17}F]fluoromethane dose was chosen to yield a count rate in striatum roughly comparable to that from [^{18}F]fallypride. The maximum count rate with both tracers present was 46 kHz.

For a third subject (monkey 1), [^{18}F]fallypride was not administered, and [^{17}F]fluoromethane was administered alone (3 MBq/s in 1 ml/s neon). In that case, [^{17}F]fluoromethane was first administered continuously while a 5 min static scan was performed at steady state. This was followed by two 12 min dynamic scans during modulated delivery.

2.4. Analysis

Sinograms were corrected for accidental coincidences, detector sensitivities, and attenuation. Images were reconstructed using filtered back projection (Hamming filter width 0.5) to voxels of 1.2 mm × 1.2 mm in-plane ×7.4 mm axial. For each monkey, eight 2.0 ml regions of interest (ROI) were specified, each ROI consisting of two adjacent cylinders having cross-sectional area 70 mm^2 and height 15 mm. For monkeys 2 and 3, two ROIs were placed on left and right striatum (LStr and RStr) defined by the observed peak of [^{18}F]fallypride concentration 85 min after injection. Six

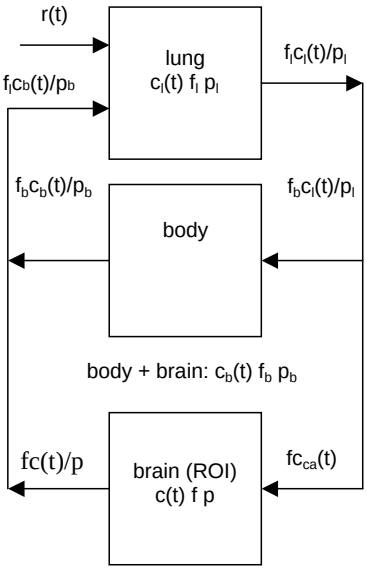

Fig. 1. Three compartment model of inhaled [^{17}F]fluoromethane kinetics showing tracer transport rates (kBq/ml/s).

ROIs were placed by eye in posterior (LPost and RPost), lateral (LLat and RLat), and frontal (LFr and RFr) regions using the dual tracer image as a guide. The set of eight ROIs for monkey 3 was coregistered manually to the images for monkey 1, for which there was no [^{18}F]fallypride scan. Whole brain (wb) ROIs of 53–62 ml were drawn in the two slices occupied by the 2 ml ROIs. Time activity curves (TACs) were generated for each ROI and each modulated delivery scan was divided into two 6 min segments for comparison purposes.

The observed TAC for a given ROI, $c_{\mathrm{ROI}}(t)$ (kBq/ml), was analyzed with an independent combination of signals from [^{18}F]fallypride, $c_{[\mathrm{F\text{-}18}]}(t)$ (kBq/ml), and [^{17}F]fluoromethane, $c(t)$ (kBq/ml),

$$c_{\mathrm{ROI}}(t) = c_{[\mathrm{F\text{-}18}]}(t) + c(t). \tag{1}$$

Given the long radioactivity and physiological time constants for [^{18}F]fallypride after initial uptake, its concentration was approximated with the average value over the course of a 6 min scan segment,

$$c_{[\mathrm{F\text{-}18}]} = \langle c_{[\mathrm{F\text{-}18}]}(t) \rangle. \tag{2}$$

In this study, there was no direct measure of the arterial input function, so the [^{17}F]fluoromethane component of the TACs was analyzed with a three compartment lung–body–brain model (Fig. 1), where "body" refers to the whole body excluding the brain ROI and lungs. The time course of tracer concentration in each compartment was assumed to follow the Fick principle, which states that change in concentration is due to addition of tracer through arterial flow and loss of tracer through venous flow and radioactive decay (Kety, 1960). Tracer concentration of blood leaving a compartment was assumed to be proportional to tissue concentration. Thus, e.g. for brain, the venous blood tracer concentration is $c(t)/p$, where p is the brain:blood partition coefficient for fluoromethane. Brain tissue concentration, $c(t)$, was modeled as

$$\frac{\mathrm{d}c(t)}{\mathrm{d}t} = fc_{\mathrm{ca}}(t) - \frac{fc(t)}{p} - \lambda c(t), \tag{3}$$

where f is the regional cerebral perfusion (ml/s ml), and $\lambda = 0.0106\,\mathrm{s}^{-1}$ is the radioactive decay rate of ^{17}F. The cerebral arterial concentration of [^{17}F]fluoromethane, $c_{\mathrm{ca}}(t)$ (kBq/ml), was modeled as the pulmonary venous concentration delayed and decayed by the lung–brain transit time, Δt (s),

$$c_{\mathrm{ca}}(t) = \frac{c_{\mathrm{l}}(t - \Delta t)}{p_{\mathrm{l}}} \mathrm{e}^{-\lambda\,\Delta t}. \tag{4}$$

Dispersion was ignored.

Input to lung tissue was assumed to have a direct component from inhaled [^{17}F]fluoromethane in the form of a constant amplitude square wave, $r(t)$ (kBq/ml/s), having a 90 s period. In addition to this, the lung compartment was fed by recirculating pulmonary arterial blood having [^{17}F]fluoromethane concentration $c_{\mathrm{b}}(t)/p_{\mathrm{b}}$, where, for ease of computation, $c_{\mathrm{b}}(t)$ is defined as the concentration of the combined body and brain compartments with p_{b} being the corresponding tissue:blood partition coefficient. Lung concentration, $c_{\mathrm{l}}(t)$, was then given by

$$\frac{\mathrm{d}c_{\mathrm{l}}(t)}{\mathrm{d}t} = r(t) + \frac{f_{\mathrm{l}}c_{\mathrm{b}}(t)}{p_{\mathrm{b}}} - \frac{f_{\mathrm{l}}c_{\mathrm{l}}(t)}{p_{\mathrm{l}}} - \lambda c_{\mathrm{l}}(t), \tag{5}$$

Body concentration was modeled as

$$\frac{\mathrm{d}c_{\mathrm{b}}(t)}{\mathrm{d}t} = \frac{f_{\mathrm{b}}c_{\mathrm{l}}(t)}{p_{\mathrm{l}}} - \frac{f_{\mathrm{b}}c_{\mathrm{b}}(t)}{p_{\mathrm{b}}} - \lambda c_{\mathrm{b}}(t), \tag{6}$$

where f_{b} is the perfusion of the combined body and brain compartments.

To more readily interpret results, initial brain, body, and lung compartment concentrations were expressed as a fraction of steady state values for continuous administration of [^{17}F]fluoromethane, i.e. $c_0 = c(0)/c(\infty)$, $c_{\mathrm{b}0} = c_{\mathrm{b}}(0)/c_{\mathrm{b}}(\infty)$, and $c_{\mathrm{l}0} = c_{\mathrm{l}}(0)/c_{\mathrm{l}}(\infty)$, with the steady state solutions to Eqs. (3)–(6) being

$$c_{\mathrm{l}}(\infty) = \frac{r/((f_{\mathrm{l}}/p_{\mathrm{l}}) + \lambda)}{1 - ((f_{\mathrm{l}}/p_{\mathrm{b}})/((f_{\mathrm{l}}/p_{\mathrm{l}}) + \lambda)) \times ((f_{\mathrm{b}}/p_{\mathrm{l}})/((f_{\mathrm{b}}/p_{\mathrm{b}}) + \lambda))} \tag{7}$$

$$c(\infty) = \frac{f}{f/p + \lambda} \times \frac{\mathrm{e}^{-\lambda\,\Delta t}}{p_{\mathrm{l}}} \times c_{\mathrm{l}}(\infty) \tag{8}$$

$$c_{\mathrm{b}}(\infty) = \frac{f_{\mathrm{b}}/p_{\mathrm{l}}}{f_{\mathrm{b}}/p_{\mathrm{b}} + \lambda} \times c_{\mathrm{l}}(\infty) \tag{9}$$

This model was used to estimate the two desired parameters for a given ROI: [^{18}F]fallypride concentration, $c_{[\mathrm{F\text{-}18}]}$ (kBq/ml), and regional cerebral blood flow (rCBF), f (ml/s/ml). The model has twelve parameters: $c_{[\mathrm{F\text{-}18}]}$, f, c_0, p, r, Δt, f_{l}, $c_{\mathrm{l}0}$, p_{l}, f_{b}, $c_{\mathrm{b}0}$, and p_{b}. Five parameters were fixed at assumed values, four were estimated by least squares fits

to a whole brain TAC, yielding the cerebral arterial input function $c_{ca}(t)$, and, finally, 2 ml ROI TACs were analyzed by least squares fitting with $c_{[F\text{-}18]}$, f, and c_0 being the free parameters. Because whole brain perfusion is set at an assumed value, the resulting value for f is a relative measure of cerebral blood flow.

Parameter values were assumed a priori as follows: Lung and body perfusion were fixed by assuming lung tissue volume, V_l, and cardiac output, F (ml/s), obey empirical scaling laws (Lightfoot, 1974).

$$V_l = 1.02 V_{l\,human} \frac{m}{m_{human}}, \tag{10}$$

and

$$F = F_{human} \left(\frac{m}{m_{human}} \right)^{0.75} \tag{11}$$

with m being the measured total body mass of each subject and representative human values being $V_{l\,human} = 0.570\,kg \times 1000\,ml/kg$ (Snyder et al., 1975), $m_{human} = 70\,kg$, and $F_{human} = 108\,ml/s$ (Leggett and Williams, 1995). With lungs receiving the entire cardiac output, lung perfusion was fixed at

$$f_l = \frac{F}{V_l}, \tag{12}$$

and perfusion of the combined body and brain compartments was assumed to be

$$f_b = \frac{F}{V_b}, \tag{13}$$

with the combined body and brain volume being total volume less lung volume,

$$V_b = m \times 1000\,ml/kg - V_l. \tag{14}$$

Tissue:blood partition coefficients for body, lung, and brain were fixed at a value measured for human brain using [^{18}F]fluoromethane and PET with arterial sampling (Koeppe et al., 1985),

$$p_b = p_l = p = 0.875. \tag{15}$$

Rather than attempt to solve the above equations analytically, a numerical approach was taken. Parameters were estimated by least squares fitting using a downhill simplex search algorithm (Press et al., 2002b). The modeled TACs were calculated iteratively in 1 s steps, and the least squares search was repeated 50 times for each TAC, each time starting at a new random location in parameter space to better locate the global minimum. For each scan, the whole brain TAC was fit with brain perfusion fixed at a typical literature value of $f = 0.48\,ml/min/ml$ (Tani et al., 1995) and with six free parameters, $c_{[F\text{-}18]}$, c_0, r, Δt, c_{l0}, and c_{b0}. The resulting parameter estimates for the amplitude of the square wave lung input, r, initial lung and body concentrations, c_{l0} and c_{b0}, and lung–brain transit time, Δt, defined the cerebral arterial [^{17}F]fluoromethane TAC, $c_{ca}(t)$, consistent with the fixed whole brain value for f. This input function, determined from the whole brain TAC, was then held fixed, and the TAC for a 2 ml ROI was fit with the free parameters being average [^{18}F]fallypride concentration, $c_{[F\text{-}18]}$, initial [^{17}F]fluoromethane concentration, c_0, and regional brain perfusion, f.

Uncertainties in the estimated parameters associated with the fitting procedure were established using a Monte Carlo bootstrap technique (Press et al., 2002a), in which 100 synthetic data sets were generated by randomly selecting points with replacement from the observed data set. The bootstrap data sets were each fit and the root mean square deviations in the fitted parameters were then taken as the uncertainties. Uncertainties in the arterial parameters, r, Δt, c_{l0}, c_{b0}, were propagated by varying each separately by its bootstrap uncertainty, fitting the 2 ml ROI TACs again, and noting the variations in the parameter estimates for $c_{[F\text{-}18]}$, f, and c_0. These variations were added in quadrature to the bootstrap parameter uncertainties for the fits to the 2 ml ROI TACs, although the error contributions from the arterial fits were relatively small. Parameter correlations were neglected in the error analysis. Sensitivities to the assumed values of whole brain perfusion, brain:blood partition coefficient, and other fixed parameters were determined by repeating the entire fitting procedure, starting with the determination of the arterial parameters. Each assumed value was varied separately, and changes were noted in the resulting values for regional brain perfusion and [^{18}F]fallypride concentration.

The continuous administration data was analyzed with the steady state solution of Eq. (3),

$$f = \frac{\lambda c}{c_{ca} - c/p}. \tag{16}$$

The steady state arterial concentration was determined by rearranging Eq. (16) and inserting the observed steady state whole brain [^{17}F]fluoromethane concentration, c_{wb}, and the assumed whole brain perfusion, $f_{wb} = 0.48\,ml/min/ml$:

$$c_{ca} = c_{wb} \left(\frac{\lambda}{f_{wb}} + \frac{1}{p} \right). \tag{17}$$

A Logan reference region analysis was performed on the [^{18}F]fallypride scans for monkeys 2 and 3 from 40 to 90 min after injection with the four lateral and posterior 2 ml ROIs used as the reference region (Christian et al., 2000; Logan et al., 1996). The resulting distribution volume ratio and an exponential fit to the reference region TAC were used to extrapolate forward and estimate the expected striatal [^{18}F]fallypride concentration at the times of the dual tracer scans.

3. Results

ROIs and corresponding TACs for a 6 min scan with [^{18}F]fallypride and [^{17}F]fluoromethane are shown in Figs. 2 and 3. Parameter estimates from the fitting

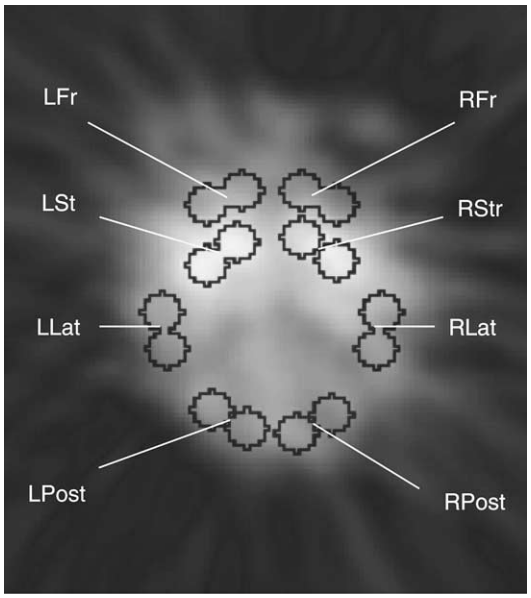

Fig. 2. Axial slice including striatum showing ROIs. Summed image over 12 min of modulated delivery of [^{17}F]fluoromethane 99 min post-injection of [^{18}F]fallypride (monkey 3).

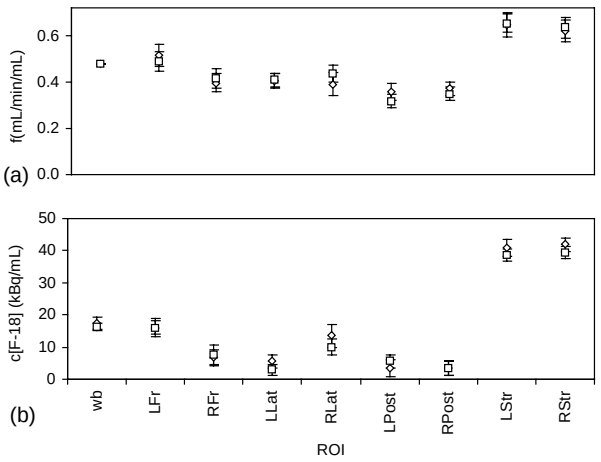

Fig. 4. Observed rCBF (a) and [^{18}F]fallypride concentration (b) from two consecutive 6 min scans during modulated delivery of [^{17}F]fluoromethane (◇) 117 min and (□) 123 min post-injection of [^{18}F]fallypride (monkey 3). Whole brain perfusion fixed at 0.48 ml/min ml.

procedure are given in Table 1, and Fig. 4 shows the measured rCBF and [^{18}F]fallypride concentrations from scans using [^{18}F]fallypride and [^{17}F]fluoromethane together.

3.1. Blood flow

The precision of the dual tracer rCBF measure can be judged by comparing results from consecutive 6 min scan segments (f_1 and f_2, Fig. 4). Averaging over eight ROIs and four pairs of consecutive scan segments (two monkeys ×

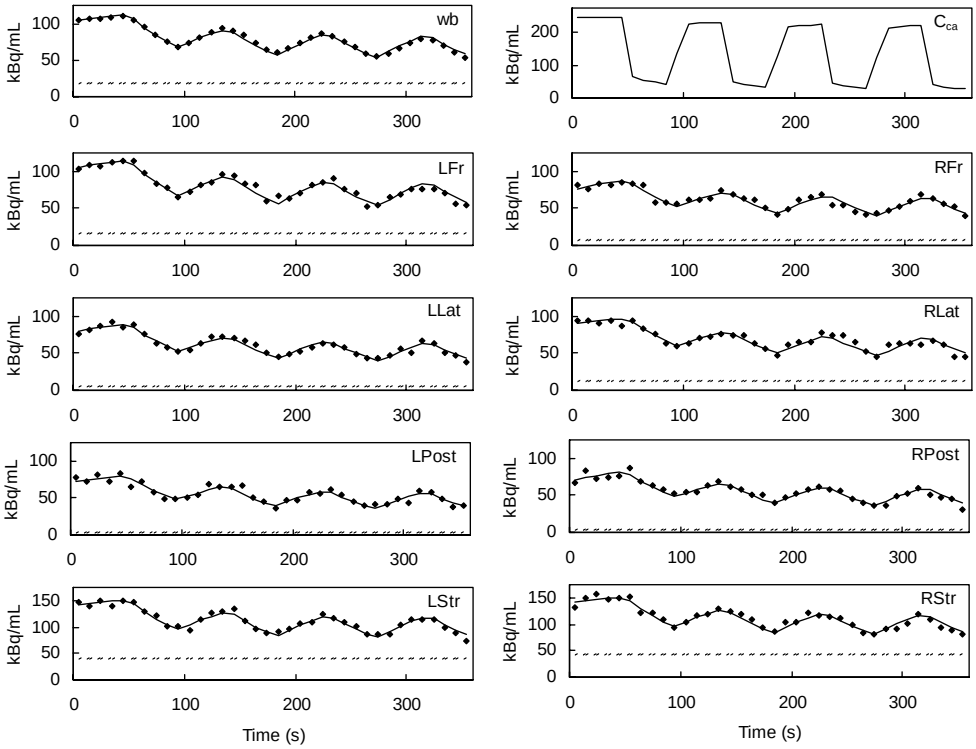

Fig. 3. Six minutes scan segment during modulated delivery of [^{17}F]fluoromethane, 117 min post-injection of [^{18}F]fallypride (monkey 3). (wb) Whole brain TAC. (c_{ca}) modeled cerebral arterial input function from fit to wb TAC. (LFr, RFr, . . . , RStr) TACs for 2 ml ROIs shown in Fig. 2 fit using $c_{ca}(t)$. (◆) Observed radioactivity, (—) modeled total radioactivity, (- - -) modeled [^{18}F]fallypride radioactivity. Note that the TACs begin high and gradually decline because this scan segment was preceded by ca. 3 min continuous [^{17}F]fluoromethane delivery.

Table 1
Parameter estimates for two consecutive 6 min scans with modulated delivery of [^{17}F]fluoromethane, 117 min (scan 1) and 123 min (scan 2) post-injection of [^{18}F]fallypride (monkey 3)

Scan	ROI	Cerebral arterial parameters from fits to whole brain TACs							
		r (kBq/ml/s)	±	Δt (s)	±	c_{l0}	±	c_{b0}	±
1	wb	71.9	2.5	2.62	0.61	1.00	0.10	1.00	0.00
2	wb	71.4	1.6	3.20	0.30	0.00	0.31	0.38	0.08
		[^{18}F]fallypride concentration and rCBF estimates							
		$c_{[F\text{-}18]}$ (kBq/ml)	±	f (ml/min/ml)	±	c_0	±		
1	wb	17.5	2.0	0.480	0.000	0.85	0.02		
	LFr	16.0	2.8	0.515	0.047	0.85	0.04		
	RFr	6.7	2.5	0.395	0.039	0.77	0.05		
	LLat	5.5	2.0	0.404	0.033	0.81	0.04		
	RLat	13.5	3.5	0.391	0.050	0.85	0.07		
	LPost	3.5	2.6	0.357	0.038	0.80	0.06		
	RPost	3.2	2.3	0.371	0.030	0.77	0.07		
	LStr	40.9	2.6	0.644	0.053	0.85	0.05		
	RStr	42.0	2.1	0.619	0.047	0.88	0.07		
2	wb	16.3	1.1	0.480	0.000	0.38	0.03		
	LFr	16.0	2.1	0.490	0.041	0.37	0.03		
	RFr	7.5	3.0	0.415	0.041	0.35	0.05		
	LLat	2.9	1.8	0.409	0.028	0.44	0.02		
	RLat	10.0	2.4	0.434	0.037	0.37	0.02		
	LPost	5.6	2.1	0.317	0.031	0.37	0.03		
	RPost	3.5	2.2	0.349	0.027	0.40	0.02		
	LStr	38.6	1.8	0.654	0.040	0.41	0.03		
	RStr	39.4	1.9	0.634	0.043	0.40	0.03		

Initial lung and body concentrations (c_{l0} and c_{b0}) are high for scan 1 due to the preceding ca. 3 min of continuous [^{17}F]fluoromethane delivery. Whole brain perfusion fixed at 0.48 ml/min/ml.

two 12 min scans), the difference in measured rCBF was Avg.$(f_2/f_1 - 1) = 3.6 \pm 11.0\%$ (S.D., $n = 32$), and the absolute difference was Avg.$(|f_2/f_1 - 1|) = 8.9 \pm 7.3\%$ (S.D., $n = 32$). The rCBF model was validated by scanning one subject (monkey 1) with [^{17}F]fluoromethane alone (Fig. 5). The results of a 5 min steady state scan were compared with four subsequent 6 min modulated delivery scan segments over eight 2 ml ROIs. The mean difference between the measures of rCBF using modulated delivery (f_{md}) and steady state (f_{ss}) was Avg.$(f_{md}/f_{ss} - 1) = 3.6 \pm 14.7\%$ (S.D., $n = 32$) and the mean absolute difference was Avg.$(|f_{md}/f_{ss} - 1|) = 12.5 \pm 8.2\%$ (S.D., $n = 32$).

To check the stability of the dual tracer rCBF measure over time, the results for pairs of 6 min scan segments were averaged and these results for the two 12 min scans (f_A and f_B) were compared. Averaging over eight ROIs and two monkeys (2 and 3), the difference in measured rCBF was Avg.$(f_B/f_A - 1) = 4.2 \pm 18.4\%$ (S.D., $n = 16$), and the magnitude of the difference in measured rCBF was Avg.$(|f_B/f_A - 1|) = 12.3 \pm 14.0\%$ (S.D., $n = 16$). As a rough comparison of the blood flow patterns of monkeys 2 and 3, the average over all four 6 min scan segments for each monkey ($f_{\text{monkey 2}}$ and $f_{\text{monkey 3}}$) were compared over eight ROIs with the results Avg.$(f_{\text{monkey 3}}/f_{\text{monkey 2}} - 1) = 0.8 \pm 13.4\%$ (S.D., $n = 8$) and Avg.$(|f_{\text{monkey 3}}/f_{\text{monkey 2}} - 1|) = 10.7 \pm 7.1\%$ (S.D., $n = 8$).

3.2. [^{18}F]fallypride concentration

The absolute accuracy of the [^{18}F]fallypride concentration measured in the dual tracer scans was judged by

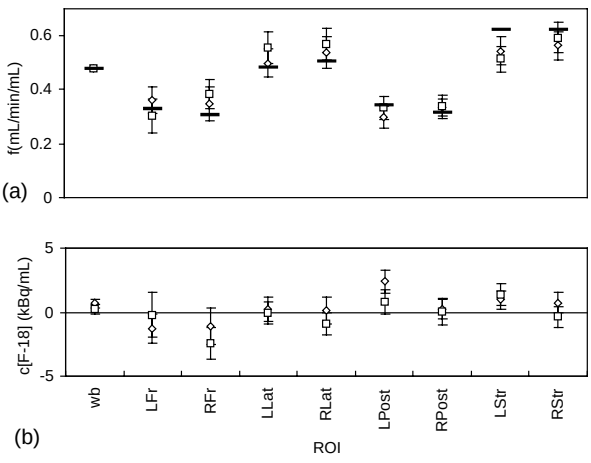

Fig. 5. (a) Comparison of modulated delivery vs. steady state measures of rCBF using [^{17}F]fluoromethane with no [^{18}F]fallypride present (monkey 1). (—) 5 min steady state scan ($t = 0$ min). Six minutes modulated delivery scan segments at (◇) 43 min and (□) 49 min. Whole brain perfusion fixed at 0.48 ml/min/ml. (b) Corresponding measures of [^{18}F]fallypride concentration (expected to be 0).

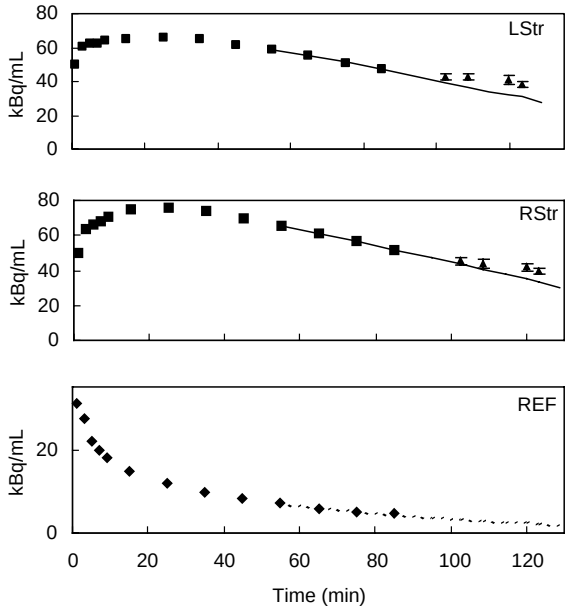

Fig. 6. Time–activity curves for [^{18}F]fallypride in left striatum (LStr), right striatum (RStr), and reference region (REF). (■) Striatal [^{18}F]fallypride measured alone, (▲) striatal [^{18}F]fallypride measured in the presence of [^{17}F]fluoromethane, (—) Logan reference region analysis extrapolated from 85 min, (◆) reference region [^{18}F]fallypride measured alone, (- - -) exponential fit to decay corrected reference region TAC. The displayed curves have not been decay corrected (monkey 3).

comparing the result for the two striatal ROIs to that expected from the preceding scan performed without [^{17}F]fluoromethane (Fig. 6). The [^{18}F]fallypride concentration measured with both tracers present was normalized to that expected based on the extrapolation of the single tracer scan: $c' = c_{[\text{F-18}]}([^{18}\text{F}]\text{fallypride} + [^{17}\text{F}]\text{fluoromethane})/c_{[\text{F-18}]}([^{18}\text{F}]\text{fallypride})$. Comparisons were performed for both monkeys, using two pairs of consecutive 6 min scan segments and the two striatal ROIs. The mean difference between the [^{18}F]fallypride + [^{17}F]fluoromethane measure and the extrapolated value was Avg.$(c'-1) = 5.0 \pm 13.0\%$ (S.D., $n = 16$) and the mean absolute difference was Avg.$(|c'-1|) = 10.6 \pm 8.8\%$ (S.D., $n = 16$). As a reproducibility check, the normalized striatal [^{18}F]fallypride concentrations measured between consecutive 6 min scans with both tracers present (c'_1 and c'_2) were compared. The mean difference was Avg.$(c'_2/c'_1 - 1) = 3.7 \pm 10.6\%$ (S.D., $n = 8$), and the mean absolute difference was Avg.$(|c'_2/c'_1 - 1|) = 7.9 \pm 7.4\%$ (S.D., $n = 8$). For the scans with no [^{18}F]fallypride present (monkey 1), the mean value of $c_{[\text{F-18}]}$ over four 6 min scan segments and eight ROIs was Avg.$(c_{[\text{F-18}]}) = 0.13 \pm 1.27$ kBq/ml (S.D., $n = 32$).

3.3. Assumptions and fitting

Table 2 shows the sensitivity to assumed parameter values based on analysis of two consecutive 6 min scans. Twenty percent variations in assumed partition coefficients and lung and body perfusion values resulted in <0.5% changes in blood flow. rCBF for the 2 ml ROIs was nearly proportional to the assumed value of whole brain perfusion. Sensitivity of the long-lived tracer concentration was greater, e.g. a 20% variation in brain partition coefficient introduced a 9% error in $c_{[\text{F-18}]}$. In the model described in Section 2.4 above, input to lung tissue from inhaled tracer was assumed to have a boxcar shape, and lung–brain dispersion was neglected. To test these assumptions, transfer of tracer from lung gas to tissue was modeled as rising and falling with an exponential time constant t_l, and the arterial input function $c_{ca}(t)$ was convolved with the dispersion function $(1/t_d)\,e^{-t/t_d}$. The estimated value of blood flow was only weakly dependent on t_l and t_d, but the measure of [^{18}F]fallypride concentration changed by 6% when the lung gas time constant was set to $t_l = 5$ s.

Local minima found in the least squares fitting procedure could yield erroneous estimated parameters. This was checked by estimating parameters for a typical 6 min dual tracer scan (monkey 3, 117 min post-injection of [^{18}F]fallypride) using varying numbers of random starting

Table 2
Changes in parameter estimates for rCBF (f) and [^{18}F]fallypride concentration ($c_{[\text{F-18}]}$) resulting from altering assumed values in the fitting procedure

Assumed parameter	Variation	Error in parameter estimates (%)							
		$\langle\Delta f_1\rangle$	S.D. ($n = 8$)	$\langle\Delta f_2\rangle$	S.D. ($n = 8$)	$\langle\Delta(f_2/f_1)\rangle$	S.D. ($n = 8$)	$\langle\Delta c_{[\text{F-18}]}\rangle$	S.D. ($n = 4$)
wb perfusion	f_{wb} + 20%	20.2	0.7	19.9	0.2	−0.2	0.5	8.5	1.5
Lung perfusion	f_l + 20%	0.0	0.0	0.0	0.0	−0.1	0.0	0.2	0.1
Body perfusion	f_b + 20%	−0.1	0.1	0.0	0.1	0.1	0.1	−4.5	1.2
Brain partition coefficient	p + 20%	−0.2	0.5	−0.1	0.2	0.1	0.4	−8.7	1.7
Lung partition coefficient	p_l + 20%	0.0	0.0	0.0	0.0	0.0	0.1	−0.3	0.1
Body partition coefficient	p_b + 20%	0.1	0.1	−0.1	0.2	−0.3	0.2	3.5	0.6
Lung gas time constant	$t_l = 5$ s	0.1	0.3	0.0	0.3	0.0	0.5	−6.5	1.5
Lung–brain dispersion	$t_d = 2$ s	0.0	0.0	0.0	0.0	0.0	0.0	0.0	0.0

Parameter estimates are from fits to consecutive 6 min TACs during modulated delivery of [^{17}F]fluoromethane 102 min (scan 1) and 108 min (scan 2) post-injection of [^{18}F]fallypride (monkey 3). rCBF sensitivities were averaged over eight ROIs for each scan segment (f_1 and f_2) and for the ratio of results (f_2/f_1). $c_{[\text{F-18}]}$ sensitivities were averaged over left and right striatum and both scan segments. In the main analysis, $t_l = 0$ s and $t_d = 0$ s (boxcar input to lung tissue and no dispersion).

parameter sets. With 1, 2, 10, and 20 starting parameter sets, the rCBF estimates for the 2 ml ROIs differed by as much as 26, 12, 0.05, and 0.03%, respectively, compared to the values reported using 50 random starting parameter sets.

4. Discussion

4.1. Reproducibility and accuracy

Comparing consecutive 6 min scans using modulated delivery of [^{17}F]fluoromethane after injection of [^{18}F]fallypride, we found reproducibility of relative rCBF measures over the eight ROIs to be 9% (Fig. 4). Without a measure of the [^{17}F]fluoromethane input function such as arterial sampling, a number of assumptions were required in modeling the data. In particular, the rCBF estimates for the 2 ml ROIs were proportional to the assumed value for whole brain blood flow. Other assumed values added only small uncertainties to the measured relative rCBF values (Table 2). Insensitivity of rCBF to some of the assumed values, e.g. brain:blood partition coefficient, is in part due to the use of a fixed value for whole brain perfusion in the analysis. Comparisons of striatal [^{18}F]fallypride concentration measured during consecutive dual tracer scans yielded 8% reproducibility, which is worse than the 1% variability between the preceding 10 min frames with only [^{18}F]fallypride present (Fig. 6).

We validated the dynamic analysis of rCBF using modulated delivery by comparing the results to those for steady state in a monkey with no [^{18}F]fallypride present. Under these conditions, the techniques agreed to within 4% (Fig. 5). In comparing the modulated delivery results to the steady state scan, it should be noted that the modulated delivery analysis was relatively insensitive to the assumed value of brain:blood partition coefficient, p (Table 2), but a 20% variation in p altered the magnitude of rCBF by 2% in the steady state analysis of the eight ROIs. We assessed the accuracy of the dual tracer method for measuring the [^{18}F]fallypride concentration by comparing the results to the extrapolated values from the preceding single tracer scans (Fig. 6). Averaging over the results for monkeys 2 and 3, this yielded 5% accuracy, but for monkey 2 the dual tracer measure of [^{18}F]fallypride concentration was low by 5% and for monkey 3 it was high by 15%. This may reflect sensitivity to some of the assumed parameter values, such as whole brain perfusion and brain:blood partitition coefficient (Table 2).

While these results demonstrate the validity of the technique, some limitations of this study should be noted. Technical constraints prevented blood sampling, necessitating the use of the fluoromethane kinetics model with a number of assumed parameters. The simplifying assumption of a single body compartment used therein may not adequately account for the different flow rates in various parts of the body. Statistical uncertainties in the parameter estimates were calculated using a bootstrap method, but they might have been more directly determined using variance images to assign uncertainties to the TACs and applying a Monte Carlo simulation. Also, measuring [^{18}F]fallypride concentration immediately before and after the [^{17}F]fluoromethane delivery would have provided a better validation of the measured concentration during the dual tracer scans. The original goal in the development of this method was to continuously monitor rCBF in the presence of a varying neurochemical tracer background, which is why a modulated delivery protocol was pursued. A post hoc simulation suggests that the optimal delivery pattern to minimize statistical noise may be a single bolus rather than the continuously modulated pattern used here.

4.2. Applications

This method may be used to study acute neurochemical changes and accompanying changes in rCBF. The proof of principle measurement reported here used the receptor ligand [^{18}F]fallypride, which is expected to yield a stable measure of dopamine D2 receptor density (Mukherjee et al., 1997). Studies of neurochemical function may make use of ligands that are more vulnerable to competition from endogenous neurotransmitters. For example, [^{11}C]raclopride can provide a relatively rapid and sensitive measure of change in the level of synaptic dopamine (Breier et al., 1997). While the present study made use of the blood flow tracer [^{17}F]fluoromethane, [^{10}C]CO_2 ($t_{1/2}$ 19.2 s) might serve as well (Schueller et al., 2001), and, if only a single bolus is delivered, it may be feasible to use the longer lived tracer [^{15}O]water ($t_{1/2}$ = 122 s) (Raichle et al., 1983). It may be possible to more accurately measure the long-lived tracer concentration by obtaining a better measure of the arterial input function, e.g. blood sampling, or by altering the flow tracer delivery pattern. Otherwise, it may be desirable to correlate rCBF with the long-lived tracer concentration measured immediately before administration of the flow tracer. Long-lived tracer concentration could also be measured to high accuracy ca. three half-lives after delivery of the short lived tracer, i.e. 3 min for [^{17}F]fluoromethane or 6 min for [^{15}O]water. Estimation of the long-lived component of the dual tracer signal would benefit from a more detailed model than that used in the present study, i.e. radioactive decay could be accounted for and additional parameters may be added to model clearance from tissue and variation in receptor binding.

We propose to correlate dopamine D2 receptor occupancy in a human subject with [^{17}F]fluoromethane measurement of rCBF at 20, 35, and 50 min post-injection of a [^{11}C]raclopride bolus (Fig. 7). The expected radiation dose from such a scan is 1.3 mSv due to 1200 MBq inhaled [^{17}F]fluoromethane (Schueller et al., 2001) and 1.1 mSv from 250 MBq injected [^{11}C]raclopride (Glatting et al., 2001). Other experimental protocols might include bolus plus infusion administration of the neurochemical tracer (Carson et al., 1997). It may be possible to correlate

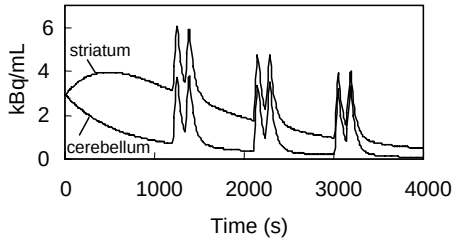

Fig. 7. Sketch of a proposed [^{11}C]raclopride and [^{17}F]fluoromethane experiment in a human subject. Pairs of 200 MBq [^{17}F]fluoromethane pulses delivered at 1200, 2100, and 3000 s following injection of a 250 MBq [^{11}C]raclopride bolus.

changes in neurochemical function and rCBF, induced by drugs, stimulation, or tasks, with 5 min temporal resolution.

Compared to other methods for simultaneous imaging of rCBF and neurochemical function (El Fakhri et al., 2001; Logan et al., 1994; Slates et al., 1999) the technique presented here is advantageous in that it provides a combination of high sensitivity to blood flow along with good spatial and temporal resolution using commercially available scanning apparatus.

This method might be applied to other neuromodulatory circuitry besides the dopaminergic system. For instance, rCBF might be correlated with serotonin receptor occupancy using [^{18}F]FPWAY (Carson et al., 2001) or [^{18}F]MPPF (Zimmer et al., 2002). Variations in blood flow could be correlated with neurochemical measures beyond receptor occupancy, such as neurotransmitter synthesis. The method might also help clarify the underlying mechanisms responsible for [^{11}C]raclopride's response to dopamine release. Modeling has shown that alterations in rCBF can mimic changes in binding, although this is more pronounced for ligands with high permeabilities, such as [^{11}C]cocaine (Logan et al., 1994). It has also been suggested that the time to reach equilibrium (Gatley et al., 2000) and receptor internalization (Laruelle and Huang, 2001) may play roles. Generally, the method proposed here might be applied to measure blood flow in the presence of any long-lived tracer.

Acknowledgements

M.J. Schueller and D.W. Dick provided cyclotron and scanner assistance. T.R. Oakes provided image reconstruction software. J. Mukherjee provided the tosylate precursor for [^{18}F]fallypride synthesis. AKC and KAD were supported by National Institutes of Health grants CA09206 and NS10205. MLS was supported by NIH grants AA10027 and AA10079. Support was also provided by the University of Wisconsin HealthEmotions Research Institute.

References

Breier A, Su TP, Saunders R, Carson RE, Kolachana BS, de Bartolomeis A, et al. Schizophrenia is associated with elevated amphetamine-induced synaptic dopamine concentrations: evidence from a novel positron emission tomography method. Proc Natl Acad Sci USA 1997;94:2569–74.

Carson RE, Breier A, deBartolomeis A, Saunders RC, Su TP, Schmall B, et al. Quantification of amphetamine-induced changes in [C-11]raclopride binding with continuous infusion. J Cereb Blood Flow Metab 1997;17:437–47.

Carson RE, Lang L, Wu Y, Ma Y, Der MG, Herscovitch P, et al. PET evaluation of two F-18-labeled 5-HT1A antagonists with intermediate affinity. J Nucl Med 2001;42(Suppl):395.

Christian BT, Narayanan TK, Shi B, Mukherjee J. Quantitation of striatal and extrastriatal D-2 dopamine receptors using PET imaging of [^{18}F]fallypride in nonhuman primates. Synapse 2000;38:71–9.

Dabbs KA, Converse AK, Barnhart TE, Dick DW, Larson J, Nickles RJ, et al. Visual activation using F-17-fluoromethane in rhesus monkey. J Nucl Med 2001;42(Suppl):934.

de la Fuente-Fernández R, Ruth TJ, Sossi V, Schulzer M, Calne DB, Stoessl AJ. Expectation and dopamine release: mechanism of the placebo effect in Parkinson's disease. Science 2001;293:1164–6.

El Fakhri G, Moore SC, Maksud P, Aurengo A, Kijewski MF. Absolute activity quantitation in simultaneous ^{123}I/^{99m}Tc brain SPECT. J Nucl Med 2001;42:300–8.

Gatley SJ, Gifford AN, Carroll FI, Volkow ND. Sensitivity of binding of high-affinity dopamine receptor radioligands to increased synaptic dopamine. Synapse 2000;38:483–8.

Glatting G, Nosske J, Henkel K, Neumaier B, Karitzky J, Karcher K, et al. Assessment of the radiation exposure of patients undergoing a C-11-raclopride-PET investigation. J Nucl Med 2001;42(Suppl):1038.

Huang SC, Carson RE, Hoffman EJ, Kuhl DE, Phelps ME. An investigation of a double-tracer technique for positron computerized tomography. J Nucl Med 1982;23:816–22.

Kearfott KJ. Feasibility of simultaneous and sequentially administered dual tracer protocols for measurement of regional cerebral haematocrit using positron emission tomography. Phys Med Biol 1990;35:249–58.

Kety SS. Theory of blood–tissue exchange and its application to measurement of blood flow. Methods Med Res 1960;8:223–7.

Koepp MJ, Gunn RN, Lawrence AD, Cunningham VJ, Dagher A, Jones T, et al. Evidence for striatal dopamine release during a video game. Nature 1998;393:266–8.

Koeppe RA. 2003, personal communication.

Koeppe RA, Holden JE, Polcyn RE, Nickles RJ, Hutchins GD, Weese JL. Quantitation of local cerebral blood flow and partition coefficient without arterial sampling-theory and validation. J Cereb Blood Flow Metab 1985;5:214–23.

Koeppe RA, Raffel DM, Snyder SE, Ficaro EP, Kilbourn MR, Kuhl DE. Dual-[^{11}C]tracer single-acquisition positron emission tomography studies. J Cereb Blood Flow Metab 2001;21:1480–92.

Laruelle M. Imaging synaptic neurotransmission with in vivo binding competition techniques: a critical review. J Cereb Blood Flow Metab 2000;20:423–51.

Laruelle M, Huang Y. Vulnerability of positron emission tomography radiotracers to endogenous competition: new insights. Q J Nucl Med 2001;45:124–38.

Leggett RW, Williams LR. A proposed blood circulation model for Reference Man. Health Phys 1995;69:187–201.

Lightfoot EN. Scaling and dimensional analysis in biological systems. In: Transport phenomena and living systems: biomedical aspects of momentum and mass transport. New York: Wiley; 1974. p. 347–57.

Logan J, Fowler JS, Volkow ND, Wang GJ, Ding YS, Alexoff DL. Distribution volume ratios without blood sampling from graphical analysis of PET data. J Cereb Blood Flow Metab 1996;16:834–40.

Logan J, Volkow ND, Fowler JS, Wang GJ, Dewey SL, MacGregor R, et al. Effects of blood flow on [^{11}C]raclopride binding in the brain: model simulations and kinetic analysis of PET data. J Cereb Blood Flow Metab 1994;14:995–1010.

Meyer-Lindenberg A, Miletich RS, Kohn PD, Esposito G, Carson RE, Quarantelli M, et al. Reduced prefrontal activity predicts

exaggerated striatal dopaminergic function in schizophrenia. Nat Neurosci 2002;5:267–71.

Mukherjee J, Yang ZY, Lew R, Brown T, Kronmal S, Cooper M, et al. Evaluation of D-amphetamine effects on the binding of dopamine D-2 receptor radioligand, ^{18}F-fallypride in nonhuman primates using positron emission tomography. Synapse 1997;27:1–13.

Press WH, Teukolsky SA, Vetterling WT, Flannery BP. Confidence limits on estimated model parameters. In: Numerical recipes in *C*++. Cambridge: Cambridge University Press; 2002a. p. 694–704.

Press WH, Teukolsky SA, Vetterling WT, Flannery BP. Downhill simplex method in multidimensions. In: Numerical recipes in *C*++. Cambridge: Cambridge University Press; 2002b. p. 413–7.

Raichle ME, Martin WR, Herscovitch P, Mintun MA, Markham J. Brain blood flow measured with intravenous $H^{215}O$. Part II. Implementation and validation. J Nucl Med 1983;24:790–8.

Schueller MJ, Barnhart TE, Dabbs KA, Dick DW, Roberts AD, Nickles RJ. Whole body dosimetry of [^{14}O]H_2O, [^{10}C]CO_2, and [^{17}F]CH_3 [abstract]. J Nucl Med 2001;42(Suppl S):1044.

Slates RB, Farahani K, Shao YP, Marsden PK, Taylor J, Summers PE, et al. A study of artefacts in simultaneous PET and MR imaging using a prototype MR compatible PET scanner. Phys Med Biol 1999;44:2015–27.

Snyder WS, Cook MJ, Nasset ES, Karhausen LR, Howells GP, Tipton IH. International Commission on Radiological Protection No. 23: Report of the Task Group on Reference Man, Oxford: Pergamon Press; 1975.

Sunderland JJ, Nickles RJ. Acceptance testing of the CTI 933/04 ECAT scanner. J Nucl Med 1988;29(Suppl):880.

Tani Y, Ishihara T, Kanai T, Ohno T, Andersson J, Lilja A, et al. Effects of 6*R*-L-erythro-5,6,7,8-tetrahydrobiopterin on the dopaminergic and cholinergic receptors as evaluated by positron emission tomography in the rhesus monkey. J Neural Trans [Gen Sect] 1995;102:189–208.

Volkow ND, Wang GJ, Fowler JS, Logan J, Schlyer D, Hitzemann R, et al. Imaging endogenous dopamine competition with [^{11}C]raclopride in the human brain. Synapse 1994;16:255–62.

Zimmer L, Mauger G, Le Bars D, Bonmarchand G, Luxen A, Pujol JF. Effect of endogenous serotonin on the binding of the 5-hT1A PET ligand ^{18}F-MPPF in the rat hippocampus: kinetic beta measurements combined with microdialysis. J Neurochem 2002;80:278–86.